



# FW and Blanket Technology Development Progress at SWIP

Jiming Chen<sup>1</sup> · Xiaoyu Wang<sup>1</sup> · Pinghuai Wang<sup>1</sup> · Min Xu<sup>1</sup> · Xuru Duan<sup>1</sup> · Kun Wang<sup>2</sup> ·  
Shuqin Wu<sup>2</sup> · Fengchao Zhao<sup>1</sup> · Xiaobo Zhu<sup>1</sup> · Xinghua Wu<sup>1</sup> · Qian Li<sup>1</sup> · Hongbin Liao<sup>1</sup> · Jing Wu<sup>1</sup> ·  
Long Zhang<sup>1</sup> · Yi Zhou<sup>1</sup> · Hongxiang Zhang<sup>1</sup> · Qixiang Cao<sup>1</sup> · Weishan Kang<sup>1</sup> · Baoping Gong<sup>1</sup> ·  
Bo Yang<sup>1</sup> · Bing Zhou<sup>1</sup> · Jialin Li<sup>1</sup> · Fanya Jin<sup>1</sup> · Xingfu Ye<sup>1</sup> · Hui Gao<sup>1</sup> · Jun Wang<sup>1</sup> · Qian Sheng<sup>2</sup> ·  
Pan Huang<sup>1</sup> · Fen Wang<sup>1</sup> · Xiaoping Fan<sup>1</sup> · Hong Yang<sup>1</sup> · Zhen Leng<sup>1</sup> and SWIP Blanket Team<sup>1</sup>

Received: 26 September 2020 / Accepted: 24 February 2021

© The Author(s), under exclusive licence to Springer Science+Business Media, LLC, part of Springer Nature 2021

## Abstract

Blanket, including its first wall (FW), is one of the key components in the fusion reactor, which works in the severe condition with the huge high energy neutron irradiation, high heat flux and electromagnetic load. Facing these technical challenges for the blanket and its FW, Southwestern Institute of Physics is engaging in the development of the blanket technology following the proposed China magnetic confinement fusion development strategy. This paper presents the design and R&D progress of the ITER FW and blanket, Chinese helium cooled ceramic breeder test blanket module (HCCB TBM) for ITER and HCCB tritium blanket for China Fusion Engineering Test Reactor (CFETR). The design of the ITER enhanced heat flux FW has been updated to improve manufacturability and to reduce water leak risk. Key technologies have been qualified by high heat flux tests of small mock-ups and full-scale plasma-facing fingers. New assembly technologies are under development. Following the completion of full-scale prototype qualification, the ITER shielding blanket modules are under manufacturing for series production. The preliminary design of HCCB TBM for ITER is under implementation to improve the manufacturability and inspectability based on the fabrication study. Two prototypes of TBM submodule have been fabricated and tested to validate the feasibility of manufacture procedure, which are finally assembling into one semi-prototype of TBM. The preliminary design of HCCB tritium blanket for CFETR has been completed and the R&D has been started, especially for the special technologies different with the ITER blanket and TBM. Meanwhile, the progress of reduced activation ferritic/martensitic steel and function materials for blanket are also presented.

**Keywords** First wall · Blanket · SWIP

## Introduction

As one of the key components in fusion reactor, the tritium breeding blanket is indispensable to realize the functions of fusion power generation and tritium self-sufficiency, but it still faces a lot of technical challenges before engineering utilization, such as materials, fabrication and validation. In

order to meet these challenges, the Southwestern Institute of Physics (SWIP) is engaging in the development of the blanket technology, which is also one of the key research areas based on the near-term and medium-term goals of SWIP [1]. The main fields include the development of the structural material and functional materials for blanket, the joining technology of the first wall (FW) armor, the fabrication process, inspection and testing of blanket.

The blanket technology development at SWIP are focusing on the technologies research for the blanket based on the existing experimental facilities and platforms, which include the development of the design, materials, fabrication processes, ancillary systems, etc. At same time, SWIP,

---

✉ Xiaoyu Wang  
wangxy@swip.ac.cn

<sup>1</sup> Southwestern Institute of Physics, Chengdu, China

<sup>2</sup> China International Nuclear Fusion Energy Program  
Execution Center, Beijing, China

as an active contributor, is playing important role for the design and construction of ITER shield blanket and test blanket module (TBM) [2], which technology will be tested and verified during ITER operation. Moreover, beyond ITER, the China Fusion Engineering Test Reactor (CFETR) has been proposed by Chinese fusion community, which target is to bridge the technical gap between ITER and the future prototype fusion power plant [3, 4]. SWIP, as one of main proposer for CFETR, has started the preliminary design and pre-R&D for its tritium breeding blanket.

Currently SWIP undertakes the important projects related to the blanket technology, including the ITER FW and blanket module procurement (both for ITER shield blanket), the design and manufacture of the helium cooled ceramic breeder test blanket system (CN HCCB TBS) for ITER [5], the design and R&D of HCCB tritium breeding blanket (TBB) for China Fusion Engineering Test Reactor (CFETR) [6]. With the constantly advancing of these projects, the reduced activation ferritic/martensitic (RAFM) steel, Chinese low-activation ferritic/martensitic steel (CLF-1), has achieved 5 tons scale ingot and its industrialized fabrication process has been standardized [7]. The fabrication technologies of tritium breeder and neutron multiplier have been developed together with industries [8]. Meanwhile, the component design and fabrication, linked with these material developments, in particular the key components, such as the ITER first wall and tritium breeding blanket, are intensively studied at SWIP. Also, many fabrication, inspection and testing facilities for blanket have been constructed or planned by SWIP. This paper thus overviews the present design and R&D status of ITER FW and shielding blocks procurement packages, as well as the CN HCCB TBS, which will be tested in ITER facility, and CFETR HCCB TBB.

## ITER First Wall and Shielding Blanket Procurement

### Design Optimization of EHF First Wall

ITER first wall provides thermal shielding to the blanket shielding modules behind it and limits the plasma boundaries [9, 10]. The heat flux to the surfaces from the burning plasma is up to  $2 \text{ MW/m}^2$  for normal heat flux (NHF) FW panels and  $4.7 \text{ MW/m}^2$  for the enhanced heat flux (EHF) panels, half by half in the quantities. The FW panels must survive from 15,000 thermal cycles at the heat fluxes as it is designed as a half-life component.

To have sufficient high thermal load removal capability, the plasma facing units of the EHF FW panels employ a typically 40 mm wide and 5 mm high hypervapotron

(HVT) cooling channels in its CuCrZr/316L(N) joint structural heat sink, cooled by 4 MPa and 2 m/s water with an inlet temperature of about  $70^\circ\text{C}$ . To mitigate the magnetic forces generated in transient cases, a FW panel is divided into 40 fingers with 1 mm gap for one to the other, mounting on a 316 L(N) steel central beam as a supporting and water manifold structure. The HVT cooling channels are distributed in each of the fingers as the plasma-facing units. Vacuum hot-pressing Beryllium in the form of tiles is used as the plasma-facing material for its good-compatibility with the burning plasma and high thermal conductivity to transfer the surface heat to the heat sink. The various materials for the fingers shall be reliably kept contacting during operation for good thermal conductivity across the material joint interfaces and having good bounding strengths tolerable to the thermal stress and the coolant pressure during the 15,000 thermal cycling.

The original design of the EHF FW panel has all of the FW fingers connecting to the central beam by 15 mm thick laser welding at the bottom corner of a narrow and deep central slot of the component [9]. It makes large welding deformation and leads high risk in control of the assembly tolerance. Besides, this makes the fingers having no replaceability whenever there are failures, causing the other high manufacturing risk of the whole panel. The water connection between the fingers and the central beam uses tubes welding inside them at the bottom of two water houses, and volumetric non-destructive inspection of the welds is not accessible. This manner of water connection results in large number of covers welding on the water houses in narrow space. Most of the welds are not inspectable for the volumetric NDT. Water leak risk during ITER operation cannot be mitigated by taking measures at manufacturing phase.

The design is improved by solving these issues for better manufacturability and inspectability. As shown in Fig. 1, the fingers are assembled to the central beam mechanically

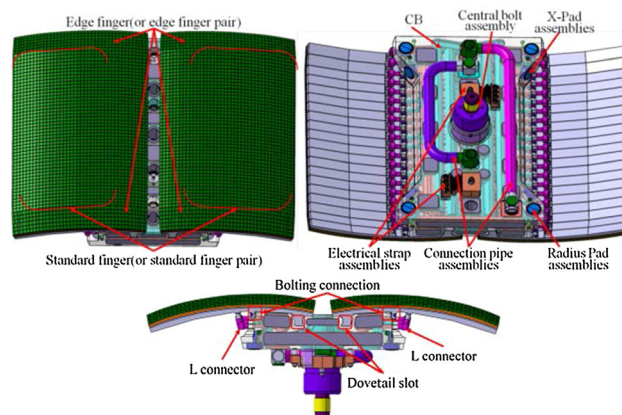
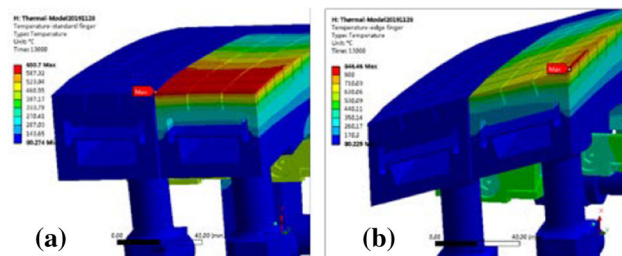


Fig. 1 3-D view of the updated FW04 panel

with a taper structure and a bolt for each finger pair. The water connection is moved to outside of the bodies by L-type pipes. As a result, the pipe can be cut for repairing if there are issues for the pipe welding and the fingers are thus replaceable. The repairing can be repeated twice with the smallest orbital TIG welding head, making the manufacturing more flexibility. The welds can be inspected by radiographic examination. Due to this change, the cover plates welding on water houses reduced largely. The number of the covers reduced from 178 to 36. The number of welds becomes much fewer for the inspection, and all is accessible for ultra-sonic examination as the space between the welds gets larger as well.

The panel is shaped in both toroidal and poloidal directions for shading the leading edge from excessive high heat flux. Accordingly, the fingers are categorized as the normal fingers (shaping toroidally) in the central area and the edge fingers (shaping bidirectionally). The normal ones have rectangular HVT cooling channels while the edge ones have to use an irregular channel with acute angle corner to accommodate the shaping. Thermal analysis shows the maximum Be surface temperature increases from 409 to 846 °C because this variation results in longer heat transfer distance at the corner. It fails to meet the design criteria of no higher than 800 °C (Fig. 2). ITER FW is designed by test, the design for these edge fingers shall be further verified by high heat flux test at the power density for the required number of cycles.

Structural analysis and fatigue performance assessment shows satisfactory results. The minimum fatigue life of the CuCrZr heat sink is  $1.87 \times 10^4$  number of cycles, locating in the edge finger beneath the  $4.7 \text{ MW/m}^2$  loading area. The minimum fatigue life appears near an access hole where the cooling cannot be well arranged for the central beam. It is well above  $2.12 \times 10^4$  number of cycles. The 2 mm thick connection pipes from the fingers to the central beam are specially addressed to reduce its leak risk from thermal fatigue damage. Figure 3 shows the total strain distributions. The thermal fatigue life is no less than  $1.23 \times 10^6$  number of cycles. All satisfies the required life of more than  $1.5 \times 10^4$  number of cycles.



**Fig. 2** The cross-sectional temperature map of the normal finger (a) and edge finger (b),  $4.7 \text{ MW/m}^2$  surface heat load on high temperature region but  $0.35 \text{ MW/m}^2$  on other areas

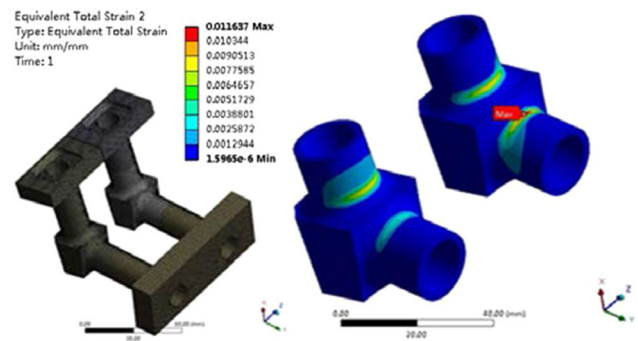


**Fig. 3** The total strain distribution in the connection pipes from the fingers to the central beam, pipe thickness: 2 mm

## Development of Key Technologies

The most challenge to manufacture the component is the bonding of tiny beryllium tiles to the CuCrZr heat sink. This technology needs to be qualified by manufacturing small mock-ups and performing cyclic high heat flux test at a specified surface power density. In 2007 six parties started a qualification program to test small mock-ups having three large Be tiles of  $80 \times 80 \times 6 \text{ mm}^3$  bonding on CuCrZr blocks with 316 L cooling tubes inside [11]. All succeeded in the high heat flux test at  $0.5 \text{ MW/m}^2$  for 12,000 cycle and  $\sim 1.4 \text{ MW/m}^2$  for 1000 cycles, including the fast brazing technology in Russian Federation and hot iso-static pressing (HIP) technologies for bonding the Be tiles in other parties. In China, the materials were bounded by HIP at 580 °C for 2 h under 150 MPa pressure. The inserting 316 L tube was bounded to two-half CuCrZr plates by HIP as well at 1040 °C for 2 h under pressure of 130 MPa.

Around 2010 the port limiter to limit the plasma boundary was cancelled, and the FW had to act as the limiter at the start-up and ramp-down of the burning plasma. The maximum surface heat flux increased by 40% for the NHF FW and by 236% for the EHF FW. For the EHF FW, the cooling channel was changed to HVT type to enhance the heat transfer from the solid CuCrZr heat sink to the 2 m/s and 4 MPa cooling water of 70 °C inlet temperature. The high heat load generated much higher thermal stress in the materials. Analysis showed the square Be tiles shall be as small as 12 mm in width to reduce the stress in the heat sink in order to meet the thermal fatigue performance requirement. The bounding of such Be tiles and the heat sink structure shall be qualified again by high heat flux test of small mock-ups in the same structure as the component at the updated surface heat load.

Small EHF FW mock-ups were manufactured in China using a combination technologies of HIP joining Be tiles to CuCrZr heat sink, explosion bonding CuCrZr to 316 L(N) steel to make bimetallic plate. The plate was



machined into HVT covers and were welded to the 316 L(N) steel base to form the HVT cooling water box by laser welding. Results showed full penetration laser welding of 5 mm wall thick HVT cooling channel with few back spattering, which is very helpful for the ITER water cooling system to mitigate radioactive material contamination and distribution around. The Be/CuCrZr and CuCrZr/316L(N) bounding interface were controlled to have good quality by NDT of ultrasonic inspection. No indication of interfacial defect higher than the echo from a 2 mm flat-bottom hole was confirmed. High Heat Flux (HHF) test of mock-ups at  $4.7 \text{ MW/m}^2$  for 7500 cycles and  $5.9 \text{ MW/m}^2$  for 1500 cycles had shown that Be tile shall be as small as  $12 \times 12 \text{ mm}^2$ , while  $51 \times 12 \text{ mm}^2$  Be tile by  $12 \times 12 \text{ mm}$  castellation was validated by a test at  $4.7 \text{ MW/m}^2$  for 16,000 cycles. Figure 4 shows the perfectness of one mock-up after the test and the uniformly distributed surface temperature in the heating phase during the thermal cycling. The HVT thermal sink survived from the test without any failure. There was no water leakage or vacuum degradation during test in the vacuum chamber. Post destructive test showed no crack at anywhere of the HVT cooling channel.

In engineering, interfacial defects at the material joint cannot be fully avoided. Analysis showed significant effect of Be/CuCrZr interface defects on local thermal stress and causing high stress concentration along the defect edge. Mechanically shear test of the joint by applying shear force at the interface showed the bounding strengths were steadily in the range of 244–259 MPa at room temperature. When a 4 mm diameter defect was placed at the interface

for an  $8 \times 10 \text{ mm}^2$  cross-sectional specimen, the measured shear strength was down to 205 MPa, which didn't show any stress concentration effect if the area was removed in the strength calculation. Similar mock-up was manufactured with 2–6 mm diameter and  $2 \times 2 \text{ mm}^2$  to  $5 \times 5 \text{ mm}^2$  square artificial defects at the bonding interface by carbon paintings before the HIP joining. High heat flux test at  $4.7 \text{ MW/m}^2$  for 5000 cycles showed that defect shall be smaller than  $12 \text{ mm}^2$  in area [12].

The EHF FW fingers for the semi-prototype (SP) has a modified HVT channel to improve thermal fatigue performance and an OF-Cu foil at the Be/CuCrZr interface for stress accommodation. The channel was modified by adding a bottom groove to lower thermal stress by reducing the rigidity of the structure. High heat flux test of two finger pairs showed acceptable results: (1) neither hot spot nor unacceptable temperature rising all over the  $4.7 \text{ MW/m}^2$  for 7500 cycles and  $5.9 \text{ MW/m}^2$  for 1500 cycling, (2) no damage of the Be tiles and hardly any deformation by the test, (3) lower than  $2.69 \times 10^{-10} \text{ Pa m}^3/\text{s}$  helium leakage rate at RT after the HHF test. Accordingly, the EHF FW design was verified. Details could be found in Refs. [12, 13].

For the latest EHF FW design, the feasibility of the pipe connection for assembling the EHF fingers to the central beam shall be demonstrated with acceptable weld quality and assembly tolerance. 19 mm diameter (OD) tubes of 2 mm wall thickness were investigated for TIG welding with the smallest OW-19 welding gun. Stable welding deformation and quality to meet the ISO 5817 level B were confirmed, including repairing the weld twice. To simulate the assembly, a number of dummy 316 L(N) Fingers, L Pipe Connectors, and a dummy central beam have been assembled through weld and then repair by twice recently. By optimizing constraining force when fitting and welding, the welding shrinkage trend to be consistent and in the level of 0.7 mm. The assembly tolerance is well controlled when keeping welding deformation reservation previously. Figure 5 is a photo of the assembly. The gaps between the fingers are well controlled in the range 1.0–1.6 mm, while the profile tolerance is 1.98 mm in maximum. All satisfy the design criteria.

There are 8 set of identical Pad assemblies on FW, which located on Radial and X position of Central Beam as shown in Fig. 1. The central beam is attached to the blanket shield block (SB) by a central bolt assembly, where low friction coating (LFC) shall be applied on the thread surface to reduce assembly torque and to avoid seizing. The central bolt preload is reacted by four Pad assemblies located in radial position, pressing the FW panel firmly onto the SB surface. Four Pad assemblies located at X position are embedded into the sides of the central beam for re-acting the radial torque, vertical and lateral forces.

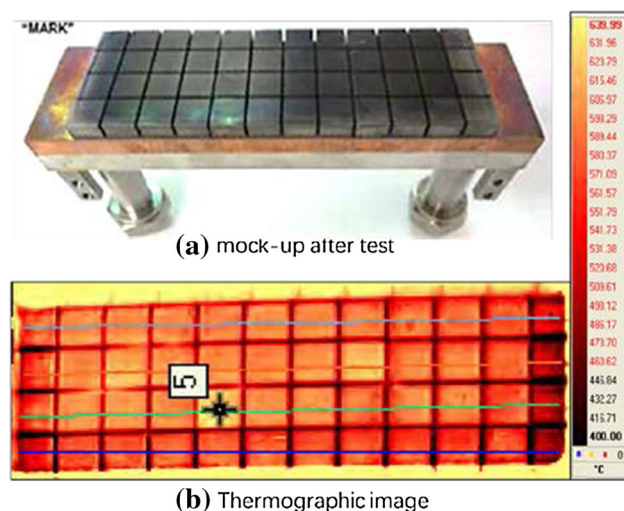


**Fig. 4** The high heat flux test of a small mock-up with  $12 \times 12 \text{ mm}^2$  Be tiles, power density:  $4.7 \text{ MW/m}^2$ . **a** After 16,000 cycles, **b** surface temperature duration heating. Results: no damage and detachment of Be tiles; no water leakage during cycling; uniform surface temperature distribution at heating



**Fig. 5** A dummy FW assembly showing the stainless-steel fingers mounted to a central beam with pipe connections

Electro-insulating coatings (EIC) is applied to the Pad surface to prevent current from flowing from them to the vacuum vessel directly but in the other circuit through the electrical strap assembly to reduce magnetic forces. The failure of the coating will increase the load on blanket and support system by orders of magnitude and may result in structural damage.

Sputtered  $\text{MoS}_2$  LFC coating on disks of the same material as the first wall components was developed, demonstrating satisfactory properties as required by ITER. To perform pin on disk wear testing according to reference standard ASTM G99-05(2010), pin and disk were manufactured from Grade 660 and Alloy 718 to represent the practical contact situation of first wall components.  $\text{MoS}_2$  coating with thickness of  $2 \pm 0.5 \mu\text{m}$  was deposited by magnetron sputtering method on all disks. All samples were subject to unilateral sliding test at maximum contact pressure (Hertz) of 1500 MPa, in Lab air,  $22 \pm 5^\circ\text{C}$ , RH  $60\% \pm 5$ , and to an accumulated sliding distance  $\geq 2$  m. Test results showed the  $\text{MoS}_2$  coating on Grade 660 and Alloy 718 completely satisfied the friction coefficient of less than 0.1.

The impact resistance of the insulation coating on pad is a big challenge. After a period of technical research, the coating was developed by plasma spraying. The Pad showed that there is no short circuit failure during 500 cycles of impact under  $450 \pm 50$  kN force. Figure 6 shows the pad before and after the impact test. Good insulation performance without any damage was confirmed. The EIC is made of  $97\% \text{Al}_2\text{O}_3 + 3\% (\text{AT}3)$ . It has thickness around  $300 \mu\text{m}$ , grain size smaller than  $15 \mu\text{m}$  and porosity

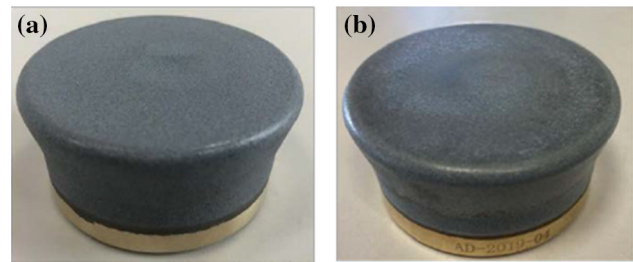


**Fig. 6** The ITER FW Pad before (a) and after (b) 500 cycles of impact test at 450kN, plasma spraying  $300 \mu\text{m}$  thick  $97\% \text{Al}_2\text{O}_3 + 3\% (\text{AT}3)$  coating on aluminum bronze pad

of less than 4.6%. Surface roughness is better than Ra  $1.6 \mu\text{m}$  after mechanical grinding. The bond strength is 30.3 MPa, much higher than the requirement of 20 MPa.

### The Design, Qualification, and Series Production of Shielding Block

The shielding block (SB) is a steel forging with inner cooling channels and outer interface features for nuclear shielding of the vacuum vessel components and the superconductor magnet. There are 440 SBs in total, and half of them are procured from China (CN). The procurement agreement (PA) execution is arranged in four main phases, including pre-PA qualification, manufacturing process qualification, series production, and delivery to the IO site. Now the Phased III is under implementation.

In order to remove the nuclear heat deposited in the SB, there is matrix of cooling channels inside, and cooling configuration is one of the main drivers for SB design. To be compatible with the interface of all the components in the vacuum vessel, the cooling channel has to be designed carefully to accommodate with the interfaces. In the central part of the SB, the cooling channels are arranged radially with frontal headers, and these channels connected to inlet and outlet openings. In the lateral parts, cooling channels are divided into several sub branches pipes in parallel, and the coolant is distributed between poloidal channels with headers located on the top/bottom of the SB surfaces. Toroidal drillings connect these sub branches with the coolant inlet and outlet openings. The cooling channels had been arranged mainly in a symmetric way to minimize the thermal distortions and stresses in the SB body. A typical SB and its cooling channel are shown in Fig. 7.

Another design driver is to reduce the electromagnetic force during off-normal events, such as major disruption and vertical displacement event. Deep poloidal and radial slits are machined to cut into the eddy current loop and mitigate the magnitude of the current. An example of SB slits configuration is given in Fig. 8. The poloidal slits are made all through the SB in the poloidal direction; they cut

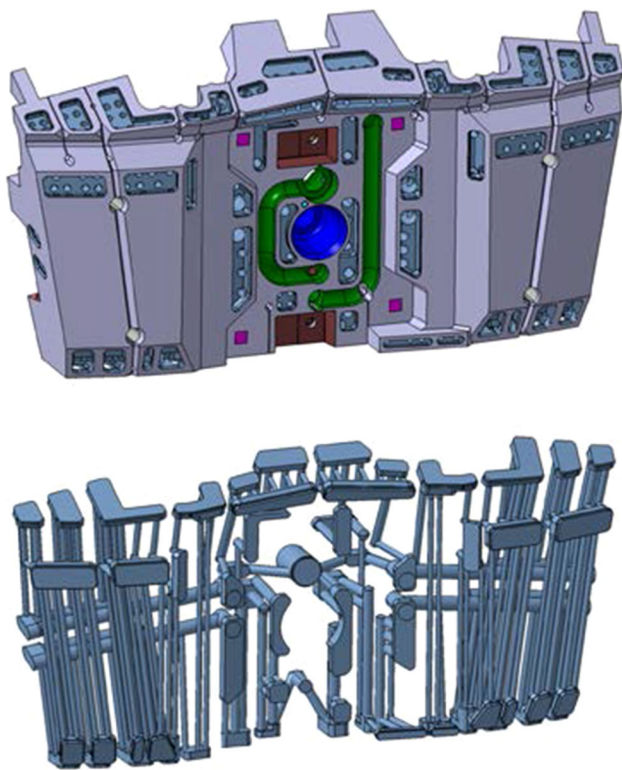


**Fig. 7** A typical SB and its cooling channels

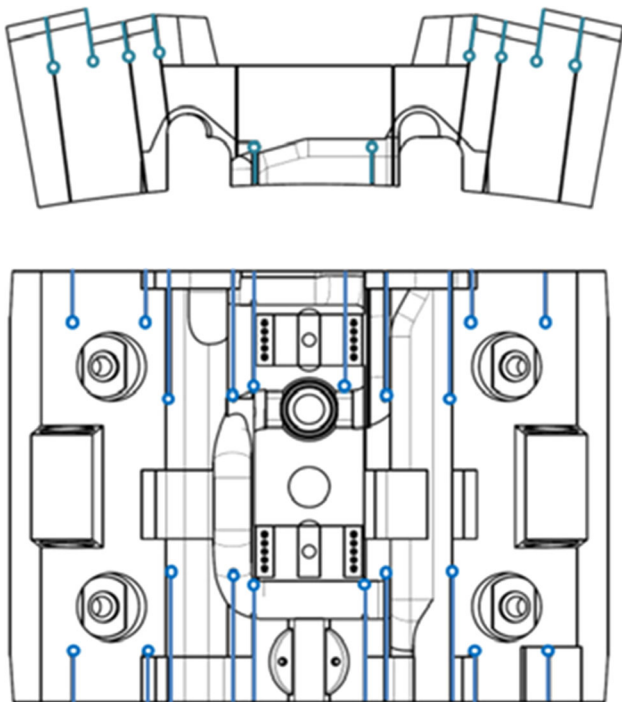


**Fig. 8** Poloidal slits (top) and radial slits (bottom) on a typical SB

into the eddy current loop caused by poloidal magnetic field changes. The radial slits are made all through the SB in radial direction. The radial slits cut into the eddy current

loop caused by radial magnetic field changes. An end hole is drilled at the end of each slit to reduce the stress concentration. The slits design is based on electromagnetic analyses results, and it can effectively control the electromagnetic loads.

During ITER operation, SB must handle a lot of loadings, including electromagnetic, thermal, coolant pressure, baking, seismic and test ones. All of the load combination has been classified, with which have been performed electromagnetic, thermal-hydraulic and thermo-mechanical analyses. The stresses obtained from analyses are evaluated with ITER Structural Design Criteria for In-vessel Components (SDC-IC) to verify whether the structure will survive from various failure modes. Optimization is needed when the local peak stress is beyond the design limit. Chamfering, removing sharp edge and adjusting local cooling channel is the frequent method to mitigate the peak stress.

An example is presented to show the design optimization for SB. The “dog leg” of SB09, where not only nuclear but also surface heat is loaded, the peak temperature will reach more than 600 °C with regular cooling configuration, see Fig. 9. A special cooling design is adopted to reduce the high temperature and peak stress, and the dimension of the water header is also carefully chosen according to the thermal–mechanical analyses, and the results are given in Table 1. According to the results, the dimension of  $t$  can be decided easily.

The fabrication is based on forging, drilling, machining and welding. Different size and angle of deep holes are drilled on a forged 316 L(N) steel block, then rough surface machining and milling of water header is followed, TIG welding is used to close the cooling circuit with 10 mm thick covers, and finally the external surface is machined. Manufacturing process qualification is aimed to test the manufacturing technology of each manufacturer, and a Full-Scale Prototype (FSP) SB09 is required to manufacture prior to the start of the series production. After completion of the FSP, a series of tests and

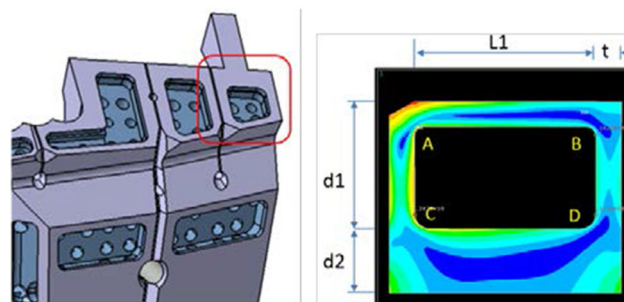


**Fig. 9** The “dog leg” of the SB09 (left) in red rectangle; 2D FE-model for the “dog leg” to study the optimized design parameter (right) (Color figure online)



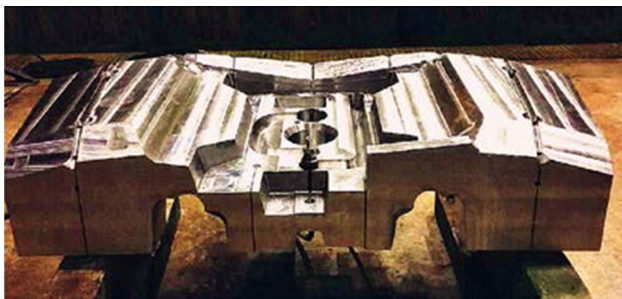
**Table 1** Peak stress (MPa) in the water header of the “dog leg” ( $d_1 = 40$  mm,  $d_2 = 20$  mm) at A–D–position with wall thickness  $t$ 

| $t$ (mm) | 8   | 10  | 12  | 14  | 16  | 20  |
|----------|-----|-----|-----|-----|-----|-----|
| A        | 488 | 456 | 420 | 382 | 347 | 253 |
| B        | 272 | 313 | 371 | 423 | 471 | 557 |
| C        | 351 | 368 | 392 | 419 | 451 | 504 |
| D        | 181 | 217 | 243 | 264 | 281 | 316 |

inspections, including inspection of geometrical shape and tolerances, ultrasonic/X-ray examination of welds, inspection of “no blocked or partially blocked water channels”, hydraulic pressure test and Hot Helium Leak Test (HHLT), are mandatory. A production of FSP SB09 is shown in Fig. 10.

To ensure the water leak tightness of the SB, hot He leak test shall be performed once on each final component, including the full-scale prototype. The test was performed after the hydraulic pressure test at  $7.15 \pm 0.2$  MPa. In order to ensure dryness, after the hydraulic pressure test, the component shall be drained and subsequently baked at 200–250 °C for a minimum of 24 h until the component cooling channel is dry. From 6 to 14 February, 2018, the HHLT was carried out.

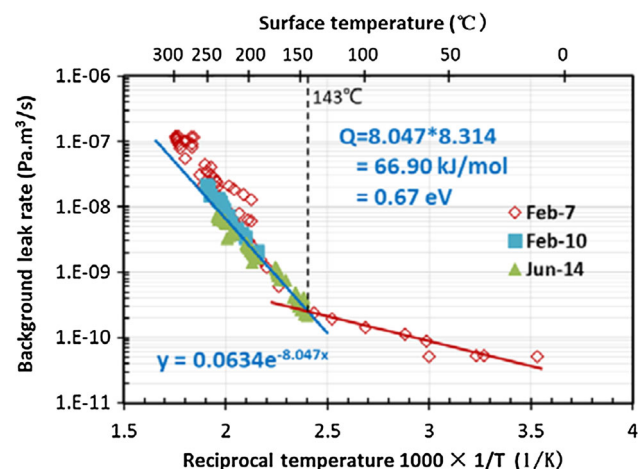
During the HHLT test of the SB09A FSP, two thermal cycles were conducted from  $\leq 80$  °C to  $250 \pm 20$  °C with two pressure cycles to 4 MPa. At the beginning of the first cycle, the helium leak test was carried out at room temperature to verify the setup and the component leak tightness, and then the SB was heated from room temperature to 250 °C to check the system sensitivity. After several trials, it turned out that the system can be calibrated with  $5 \times 10^{-10}$  Pa m<sup>3</sup>/s at temperature of 232 °C. The SB was cooled to 61 °C and the leak tightness was verified again. After the 2nd cycle, a helium leak test was carried out at 65 °C for final verification of the leak tightness of the SB. During the whole process, the vacuum of the leak test chamber was in the range of  $7.1 \times 10^{-5}$  Pa to  $1.2 \times 10^{-6}$  Pa, and the maximum temperature difference

**Fig. 10** The completion of SB09 FSP

in the SB is not exceeding 55 °C to avoid the damage by thermal stress.

The SBs are massive components in the level of 2–3 tons. They all have complex shape, large cut-out and deep slits. All these features make each of them have large volume and outer surface area, causing high thermal desorption rate of residual gases. Therefore, baking before the HHLT is very important to reach a high sensitivity of the test system. Figure 11 shows the background level during the trial test of the SB09A FSP. Clearly it follows two temperature dependences. At lower temperature than 143 °C, the leak rate increases slowly with the increasing temperature. This is assumed as the desorption of the absorbing gases at the component surface. When temperature getting higher, the rate increases much steeply, which is assumed as the volumetric releasing of hydrogen in the shield block. Residual gas analysis also showed the suddenly increasing signal of hydrogen above 150 °C. To improve the performances, the H<sub>2</sub> releasing shall be reduced.

After the accomplishment of Phase II in 2018, the SB PA execution enters in the series production in CN. Up to Sept. 2020, 194 forgings have been completed by Guizhou Aerospace Xinli Tech. Co. Ltd, and it's expected that all of the forgings will be completed within 2021. Based on the IO model delivery plan, the SB manufacturer, Dongfang Heavy Machinery Co. Ltd, has started the manufacturing with the row of SB10, SB09 and SB17. Currently, five SBs have been completed, i.e. SB10-03, 04, 06, 07, 08, and two of them were performed HHLT with acceptable results. All of SBs will be completed for its manufacturing and testing, and will be delivered to ITER site around 2024.

**Fig. 11** The background of the leak test system during the hot helium leak test of SB09A FSP

## CN HCCB TBS for ITER

### Design of CN HCCB TBS

The CN HCCB TBS project is led by the China International Nuclear Fusion Energy Program Execution Center (ITER China Domestic Agency, called CN DA), mainly with strongly supporting by SWIP, which takes the technical lead for the whole system, China Academy of Engineering Physics (CAEP) and Institute of Nuclear Energy Safety Technology (INEST). Also, many other institutes, universities and industries are involved for the design and R&D activities [5].

In 2014, China and ITER Organization signed the China HCCB TBM Agreement (CN HCCB TBMA) and China promised to fabricate and test the HCCB TBS in ITER facility, which provides the chance to validate the technical feasibility of tritium production and heat removal for blanket [2]. The conceptual design of HCCB TBS has been approved by ITER Organization in 2015 and the kick-off meeting for the preliminary design phase has been held in 2016. Now, the design optimization and R&D activities of the HCCB TBS is being implemented for the preliminary design. It is planned to hold the preliminary design review of HCCB TBS in 2022.

In order to achieve the testing objectives of the HCCB TBS, the HCCB TBS comprises several subsystems with different functions to support the testing, which includes a test blanket module set (TBM-set), a helium cooling system (HCS), a tritium extraction system (TES), a coolant purification system (CPS), a tritium accountancy system (TAS) and a neutron activation system (NAS). These subsystems are located in different rooms of the ITER buildings and connected by the connection pipes (CP). Besides, some equipment of the subsystems is located in the ancillary equipment unit (AEU) in the port cell. The pipes connecting the TBM-set with the equipment in the AEU form a pipe forest (PF) together with its structure frame. The AEU and PF are shared with the other TBS in the same port. The global layout of the HCCB TBS in the ITER building is shown in Fig. 12 [5].

Recently, the equatorial ports of ITER designated to TBSs were reduced from three to two, which meant that only four TBSs can be tested simultaneously during ITER operation. The selection of the four TBSs for the initial configuration for ITER testing is under discussion [14], which may impact the design of CN HCCB TBS due to the possible reallocation of port or possible cooperation with other ITER member.

As the core component of the HCCB TBS, the TBM-set has the duties of tritium breeding and heat generation, which consists of the test blanket module (TBM) and the

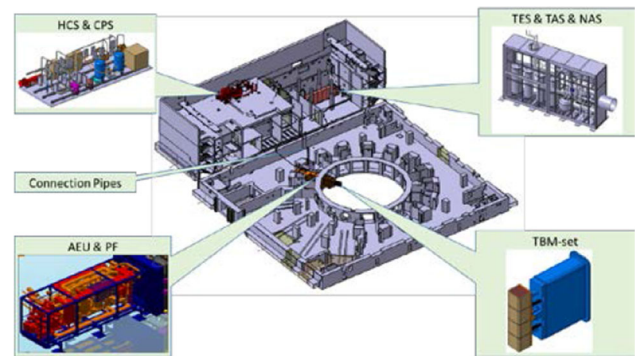


Fig. 12 Global layout of the HCCB TBS

TBM shield. It is located in the TBM frame installed in the equatorial port of the ITER vacuum vessel. The TBM directly faces plasma and produces tritium under fusion neutron irradiation, which is classified as the pressure equipment and subject to EU Pressure Equipment Directive 97/23/EC (PED). The TBM shield is just behind the TBM to provide neutron shielding and support the TBM, which belongs to the first confinement, same as the vacuum vessel, and is classified as the nuclear pressure equipment subject to the French Order dated 30 December 2015 on nuclear pressure equipment. The design and fabrication process development for both TBM and TBM shield are following the French Design and Construction Rules for Mechanical Components of Nuclear Installations (RCC-MR).

In order to meet the requirements of the tritium breeding and structure integrity under the ITER fusion operation condition, the TBM contains tritium breeding zones filled by lithium orthosilicate pebbles, neutron multiplying zones filled by beryllium pebbles and a box structure with cooling channels made by the reduced activation ferritic/martensitic (RAFM) Steel [15], as shown in the Figs. 13 and 14. Due to the TBM is recessed of 120 mm compared to the ITER shield blanket [16], the FW of TBM will be protected by the ITER shield blanket from the plasma interaction, so the armor is not requested on the FW surface of TBM. The structure of TBM is cooled by 8 MPa helium coolant provided by the HCS. The tritium breeding zones and neutron multiplying zones are purged by the 0.3 MPa helium gas with 0.1% hydrogen provided by the TES to extract the tritium produced in these zones during ITER operation phase. The tritium production ratio can achieve about 56 mg/full power day (FPD) after the design optimization for the tritium breeding zones, neutron multiplying zones and structure. Its main design parameters are given in the Table 2.

The TBM shield is also a box structure made from stainless steel 316 L(N)-IG and cooled by 4 MPa water. The pipes of TBM pass through the TBM shield and



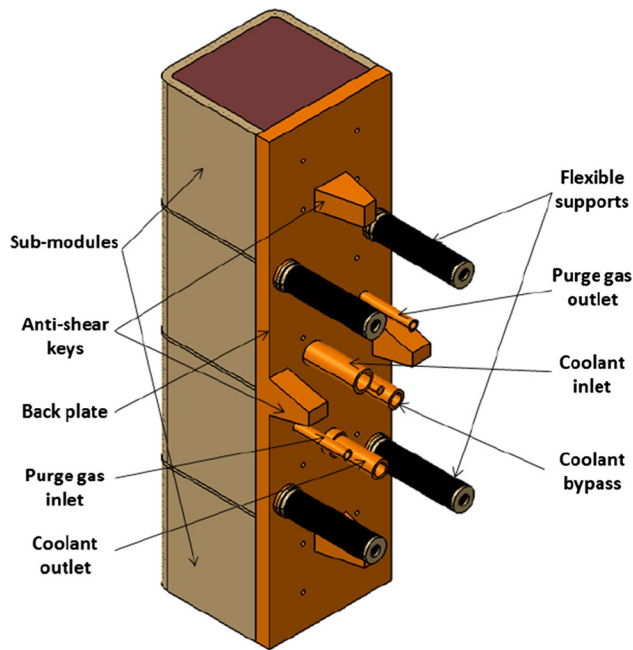


Fig. 13 TBM design

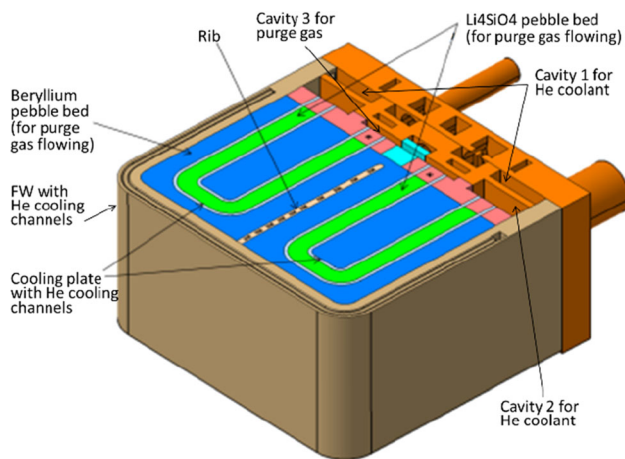


Fig. 14 Cross section view of TBM design

connect with the pipes in the PF located in the port cell [17], as shown in the Fig. 15. The internal configuration of the TBM shield has been optimized to achieve the reasonable neutron shielding effect [18].

The HCS provides 8 MPa helium gas as coolant to remove the thermal power generated in the TBM and release the heat to the ITER Components Cooling Water System-1 (for nuclear components) and its preliminary layout configuration is shown in the Fig. 16 [19]. The CPS provides the functions of coolant composition control and tritium purification from coolant. The TES extracts the tritium generated in the TBM by the 0.3 MPa helium purge gas blowing the tritium breeding zone inside the TBM [20]. The TAS monitors the tritium in the TES. The neutron

Table 2 Main parameters of HCCB TBM

| Parameters          | Values                                    |
|---------------------|---|
| Neutron wall load   | 0.78 MW/m <sup>2</sup>                    |
| Surface heat flux   | 0.3 MW/m <sup>2</sup> *                   |
| Structural material | RAFM steel (CLF-1 or CLAM)                |
| Tritium breeder     | Li <sub>4</sub> SiO <sub>4</sub> pebble   |
| Neutron multiplier  | Beryllium pebble                          |
| Coolant             | Helium (8 MPa)                            |
| Purge gas           | Helium (0.3 MPa) with 0.1% H <sub>2</sub> |
| TPR                 | 0.29 mg/pulse (450 s burn time)           |

\*The TBM is acting as a plasma facing-component but it will be recessed of 120 mm compared to the ITER shield blanket. This recess will avoid major heat loads transients on the TBM FW due to plasma instabilities which are expected in ITER but, in principle, should not be present in a DEMO [16], like CFETR

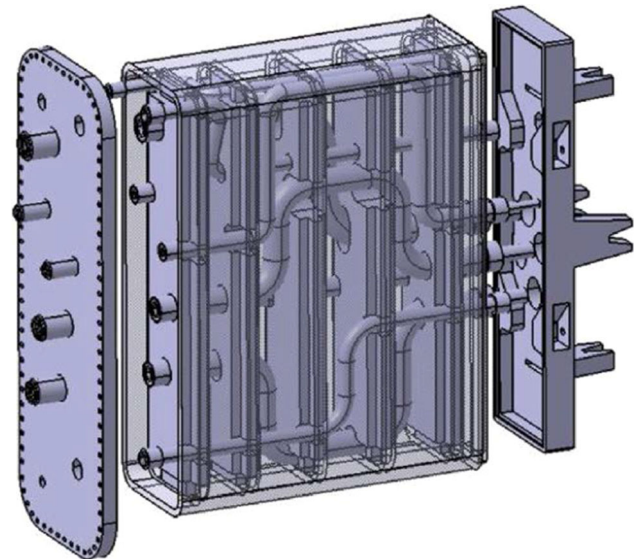


Fig. 15 TBM shield design

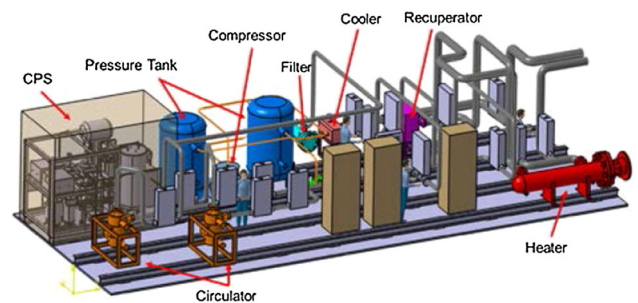


Fig. 16 Layout configuration of HCS

spectrum at the specified location in the TBM is measured by the NAS.

The preliminary designs of TBM-set and its ancillary systems have been optimized considering the system performance, safety and interface requirements. The process flow diagram (PFD) and pipe and instrumentation diagram (PID) have been prepared for all ancillary systems and their layout configurations have been updated based on the equipment investigation. Also, the system performance assessment, safety assessment and the structural analysis have been performed to verify the reasonability of the design for the HCCB TBS [15–25].

## R&D Progress for CN HCCB TBS

### Material Development

According to the ITER requirements, The RAFM steel is selected as the structural material of ITER TBM. SWIP developed the CLF-1 steel, one of the RAFM steels, for HCCB TBM together with the Institute of Metal Research, Chinese Academy of Sciences and started the industrialized trial-fabrication together with industries (Fig. 17).

Currently the technical specification of CLF-1 steel has been finalized considering the requirements of composition control, physical, thermal, mechanical, electrical, magnetic properties and so on. The industrialized fabrication procedure has been standardized based on more than 6 batches production with 5 tons scale ingots. The properties of these products satisfy the material specification. The UTS, YS and elongation are higher than 650 MPa, 550 MPa, 20% at room temperature, respectively and higher than 400 MPa, 360 MPa, 22% at 550 °C, separately (Fig. 18). The average impact energy at room temperature is larger than 200 J and the ductile brittle transition temperature (DBTT) is lower than  $-50$  °C for all the thickness CLF-1 steel products (Fig. 19) [7]. And also, the long-term high

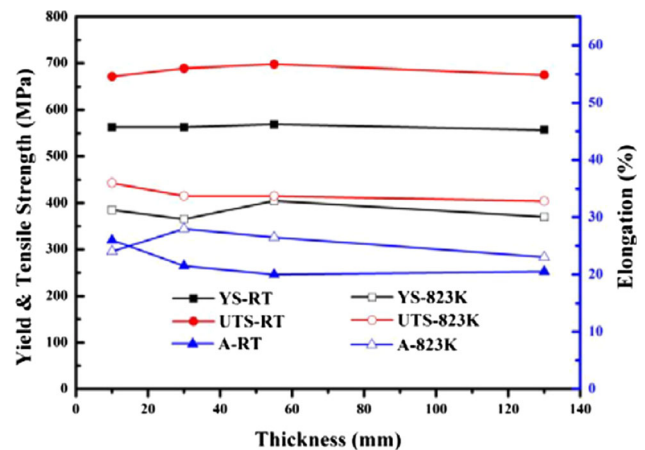


Fig. 18 Tensile properties of different thickness CLF-1 steel products (at room temperature and 550 °C)

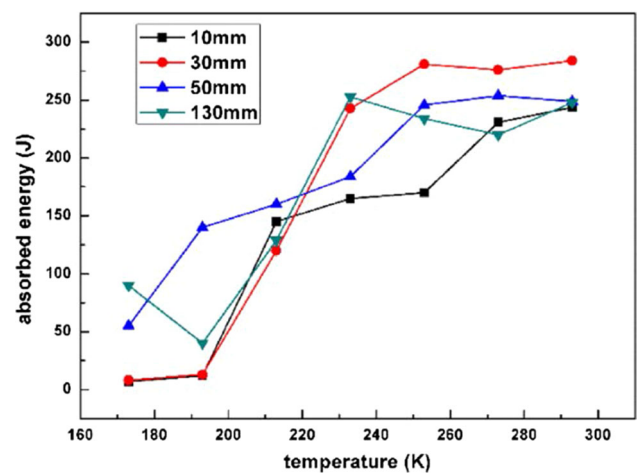


Fig. 19 Absorbed energy of different thickness CLF-1 steel products

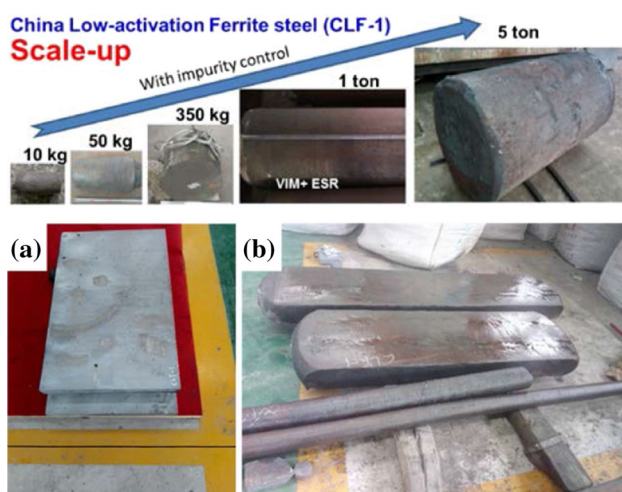


Fig. 17 CLF-1 steel development and its product

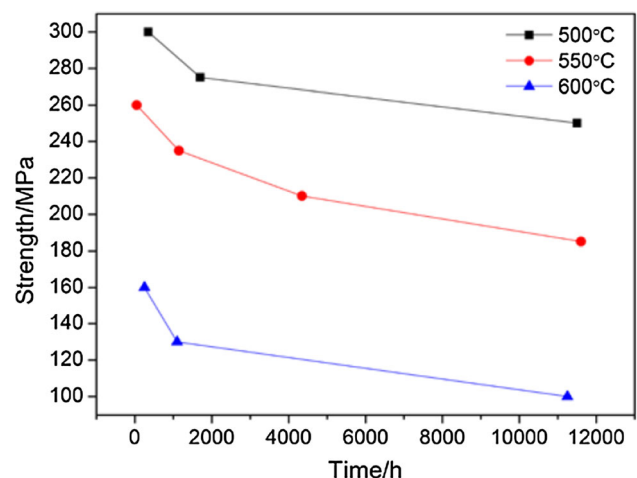


Fig. 20 The creep property of CLF-1 steel

temperature creep property of CLF-1 steel has been investigated preliminarily, which results are shown in Fig. 20, and more creep testes have been planned in the next several years.

8 tons CLF-1 plates (from 5 to 50 mm) and forgings (about 130 mm) have been fabricated and the certification requested by EU Pressure Equipment Directive 97/23/EC (PED) has been obtained under the witness of a Notified Body (NB) [7]. These materials have been used for the R&D of fabrication processes for blanket components. One Chinese nuclear industry standard and two Chinese special fusion standards have been established for the different products of CLF-1 steel.

The fabrication technique, rotation electrode process (REP), has been developed for the production of neutron multiplier beryllium pebble by SWIP together with industry and the properties have also been tested [8, 26]. Recently the fabrication facility for beryllium pebble has been updated in order to improve the product output. After the updating, the production scale has achieved  $\sim 10$  kg/batch with the properties  $\text{Be} > 98.5\%$ ,  $\text{BeO} < 1.0\%$ , pelletizing ratio  $> 60\%$  and the pebble diameter in the controllable range of 0.5–1.5 mm (Fig. 21). The helium ion implantation experiments were performed for the beryllium samples to investigate the effect of helium on the microstructure and hardness of the beryllium material. The results show that the probability of beryllium pebble crushing increase with the increase of irradiation. Also, as one of advanced options, the fabrication process for beryllium alloy is under development.

The melt spraying process is used to fabricate the tritium breeder lithium orthosilicate pebble and several batches have been fabricated by this process and tested [27]. After the optimization of fabrication process, the performance of lithium orthosilicate has been improved (Table 3), in which the crush load was crossly checked by the Karlsruhe Institute of Technology (Germany) and Institute of Plasma Research (India). Currently a new manufacture facility for lithium orthosilicate pebble is under construction and its production capacity will satisfy the requirements of CN HCCB TBM (Fig. 22).



Fig. 21 Beryllium pebble fabrication facility and product

**Table 3** Physical characteristics of  $\text{Li}_4\text{SiO}_4$  pebble

| Parameters                                      | Values          |
|---|-----------------|
| Density (% TD)                                  | $> 94$          |
| Open porosity (%)                               | $\sim 5.2$      |
| Closed porosity (%)                             | $\sim 0.75$     |
| Specific surface area ( $\text{m}^2/\text{g}$ ) | 1.095           |
| Total pore volume for pores ( $\text{cc/g}$ )   | $2.0\text{E}-3$ |
| Average crush load (N)                          | $\sim 25$       |



Fig. 22 Lithium silicate pebble and its new fabrication facility

The pebble bed technology is also one important aspect for the HCCB TBM. Currently only thermal conductivity of lithium silicate pebble bed is measured at different temperature (Fig. 23). A new multi-physics field pebble bed testing facility is under construction and it will allow to test the pebble bed properties blew by the purge gas under compress force, which will provide more precise performance data for the TBM design.

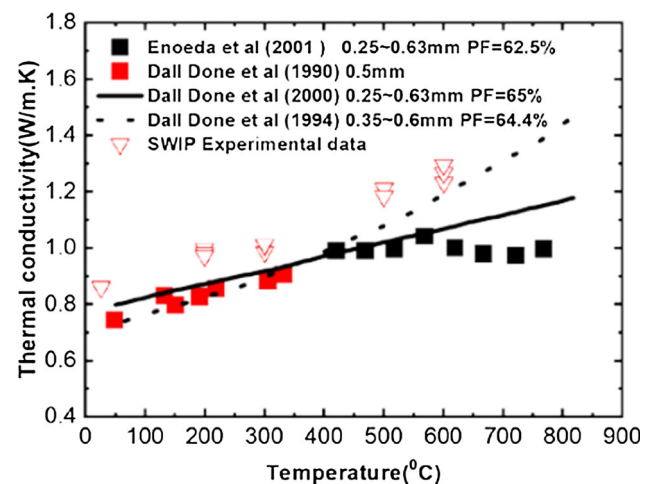


Fig. 23 Effective thermal conductivity of lithium silicate pebble bed



## Fabrication Processes

The fabrication process for CN HCCB TBM has been studied for several years. As a very complicated box structure, the fabrication technology of the TBM is one of the most important challenges to achieve the requirements of pressure equipment. Several potential welding methods have been investigated together with other industries, institutes and universities, such as tungsten inert gas welding (TIG), laser beam welding (LB), electron beam welding (EB), hot isotactic pressing welding (HIP) and vacuum hot-pressing welding (VHP). Based on the investigation and the requirements given by the RCC-MR, it is considered to use the LB welding and EB welding as the main welding methods for the fabrication of TBM, and the TIG welding as the supplementary method (Fig. 24).

For the LB welding, the CLF-1 steel welding technology for the thickness from 5 to 35 mm by single pass LB welding and narrow-gap laser beam welding process have been developed [28]. The strength at the welding joint meet the requirements, but the impact energy for the 35 mm thick welding is fluctuated, which needs deeper study for the welding and heat treatment process. The EB welding technology of CLF-1 based on 32 mm and 50 mm thickness has been studied, and the hardness and the tensile strength have been tested after the PWHT process, which meet the requirements [29]. Besides, the dissimilar welding of CLF-1/316L steel by TIG welding was studied. Due to the different properties of the two materials, the filler material (welding wire grade: ER316) was used as the transitional layer and filler material. After the PWHT, the tensile strength and impact energy of the welding joints are acceptable.

Based on the above welding method research, the prototypes of key components including first wall, cooling plate, back plate, breeding unit, etc., have been fabricated (Fig. 25) and tested. Using these components, a semi-



Fig. 24 Welding technology development

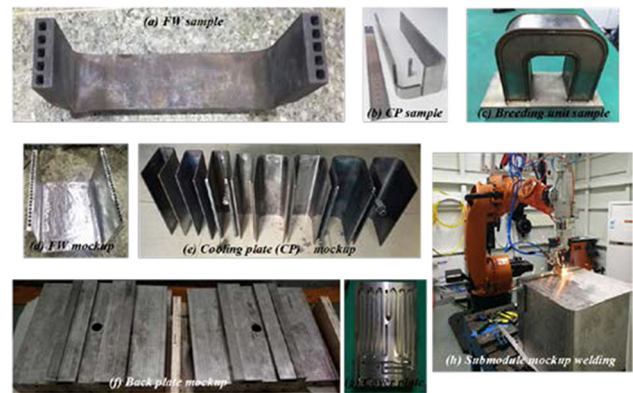


Fig. 25 TBM fabrication technology development

prototype of TBM module has been assembled and tested, which verified the feasibility of these fabrication processes for the TBM. During the fabrication, the non-destructive inspections were implemented, and after that, the leakage and pressure testing are mandatory for these TBM components. The current testing results show at least  $1\text{E}-8\text{ Pa/m}^3$  leakage rate can be achieved and the components can bear up to 22 MPa pressure testing without obvious deformation and damage, which basically verify the reasonability of the current fabrication processes for HCCB TBM.

In order to verify the thermohydraulic performance of TBM components, one small helium cooling experiment loop (HeCEL-1) has been constructed and operated by SWIP. Its operation pressure and helium flow rate are 8 MPa and 0.1 kg/s, respectively. The operation temperature at experimental section can achieve  $400\text{ }^{\circ}\text{C}$  [30]. The ITER Mini-CODAC, as the simulation environment of ITER control framework, was connected with the HeCEL-1 loop and realized the monitoring and control functions of the HeCEL-1. The HeCEL-1 loop is also connected with the 60 kW high heat flux testing (HHFT) facility (EMS-60), as shown in Fig. 26. Base on this platform, the hydraulic test of breeding unit and the high heat flux test of FW sample can be carried out.

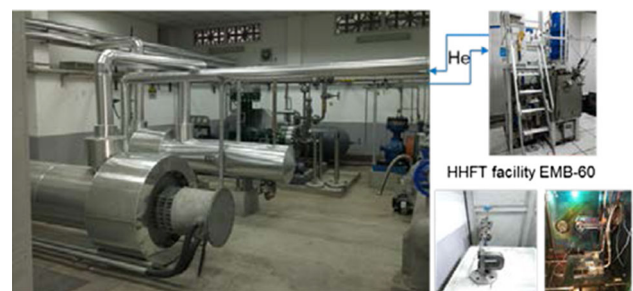


Fig. 26 HeCEL-1 loop and its experiments

## CFETR HCCB TBB

### Design Status of CFETR HCCB TBB

CFETR conceptual design has been started since 2011 under the support of the Ministry of Science and Technology (MOST) of China and managed by the China International Nuclear Fusion Energy Program Execution Center. Now the main design parameters of the CFETR are finalized and the pre-engineering design is under development [4].

The pre-engineering design and R&D of TBB for CFETR were started from 2017, which covered the HCCB TBB and WCCB TBB. The design of HCCB TBB is being developing by SWIP with close cooperation among several domestic institutes and universities, mainly including the Institute of Plasma Physics of Chinese Academy of Science (ASIPP) and the University of Science and Technology of China (USTC).

The design objectives of the HCCB TBB system for the CFETR are tritium breeding ratio (TBR)  $\geq 1.1$  and satisfy the functions of heat removal and neutron shielding under the conditions to ensure the safety, structural integrity of TBB and the compatibility with the CFETR design. The HCCB TBB system includes HCCB TBB, primary helium cooling system (HCS) with interface with the tritium plant, second cooling loop and other services, as shown in the Fig. 27 [6].

The preliminary profile and layout configuration of CFETR TBB has been obtained after iteration with plasma physics, which is consistent for both the HCCB TBB and WCCB TBB. The CFETR TBB utilizes the “banana” segment design that is compatible with the strategy of the remote handling (RH). There are two inboard segments and three segments for each VV sector, as shown in the Fig. 28. Each segment comprises several blanket modules with 20 mm gap at front and connected as one segment at the back plate. Totally, the CFETR TBB comprises 80 blanket

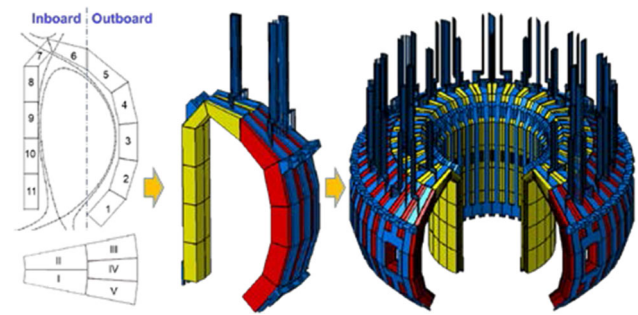


Fig. 28 Layout configuration of CFETR TBB

segments, containing about 432 blanket modules, and total weight is more than 5000 ton.

The current HCCB TBB design selects tungsten (or tungsten alloy) as the armor material for the first wall, oxide dispersion strengthened (ODS) steel or/and RAFM steel as the structure materials, lithium silicate (or lithium titanate) as tritium breeder, beryllium (or beryllium alloy) as neutron multiplier, as shown in Table 4.

The blanket module uses the integrated design for both breeding and shielding functions, which includes four zones, breeding zone, distribution zone, shielding zone and manifold (Fig. 29). The breeding zone, with the most important functions of tritium breeding and main heat generation, includes the tritium breeder, the neutron multiplier and the box structure with cooling channels inside and the tungsten armor on the first wall surface. 12 MPa helium coolant flows through the cooling channels and removes the thermal energy due to the heat flux coming from plasma and the nuclear heating. Purge gas (0.3 MPa helium with 0.1%  $H_2$ ) blows the breeder to extract the tritium generated in it. The distribution zone is used to distribute the helium coolant for the breeding zone. The neutron shielding is the main function of the shielding zone, which is cooled by water, similar to the VV. The

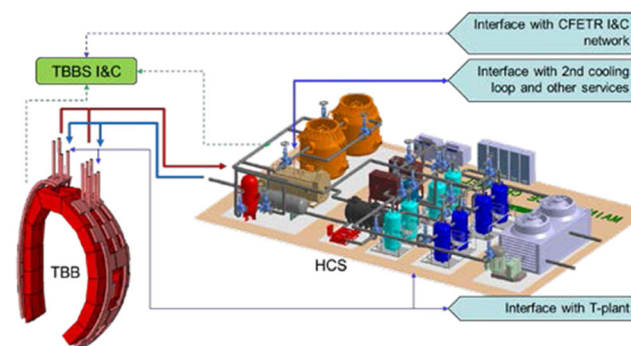


Fig. 27 Schematic configuration of HCCB TBB system

Table 4 Main parameters of HCCB TBM

| Parameters                 | Values                    |
|----------------------------|---------------------------|
| Neutron wall load          | $\sim 1.7 \text{ MW/m}^2$ |
| Surface heat flux          | $\sim 0.5 \text{ MW/m}^2$ |
| FW armor                   | W/W alloy                 |
| Structural material        | ODS RAFM + CLF-1          |
| Tritium breeder            | $Li_4SiO_4/Li_2TiO_3$     |
| Neutron multiplier         | Be/Be alloy               |
| Purge gas                  | He with 0.1% $H_2$        |
| Coolant for breeding zone  | He (12 MPa)               |
| Coolant for shielding zone | Water                     |
| TBR                        | $> 1.1$                   |

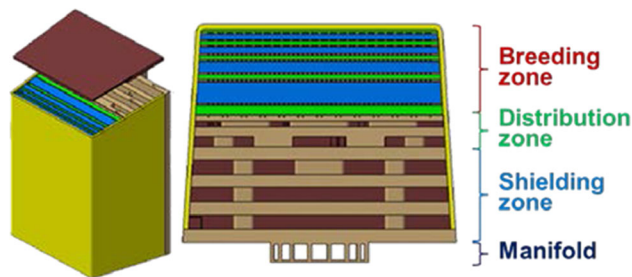


Fig. 29 Blanket module design of HCCB TBB

manifold is to carry the coolant and purge gas from the main pipes located at upper ports to each blanket module. Currently, the RCC-MR is used as the design code for CFETR HCCB TBB.

The preliminary neutronics, thermohydraulic, structural assessments have been performed. The results show this preliminary design can meet the requirements of material and structural integration [31]. Recently the design of HCCB TBB focuses on the detail design optimization considering the TBR and shielding performance taking into account the neutral beam injection (NBI) ports. Based on the detail neutronics analysis model of CFETR (Fig. 30), the preliminary neutronics assessment shows that three NBI ports will result in about 5% reduction of TBR (Table 5), the fast neutron flux to toroidal field (TF) coils and its nuclear heating are under the limit after the design optimization. The size of NBI ports, the cutout size for diagnostics and the enhancement of neutron shielding are under discussion together with machine integration of the CFETR.

The preliminary safety assessments have also been performed for HCCB TBB system under several typical accidents requested by CFETR safety requirements, such as tritium release during normal operation, in-box LOCA, in-vessel LOCA, ex-vessel LOCA, LOFA (Loss of Flow Accident) and LOCA of tritium extraction system. The

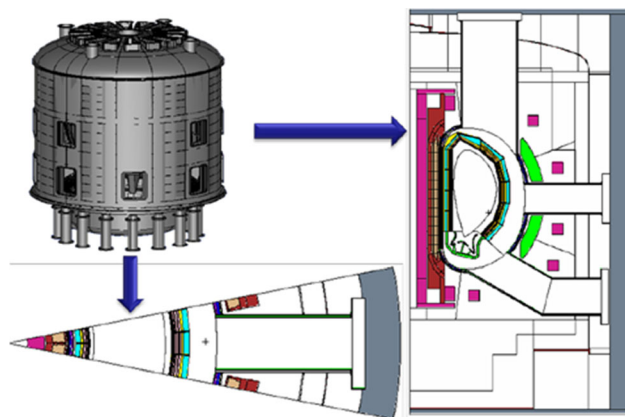


Fig. 30 Neutronics model of CFETR with HCCB TBB

Table 5 NBI ports impact to TBR

| Number of NBI port (3 m × 2 m) | TBR  |
|--------------------------------|------|
| No NBI port                    | 1.16 |
| Two NBI ports                  | 1.13 |
| Three NBI ports                | 1.11 |

results show that the structure integrity can be kept during LOFA and the irradiation release is controllable with the suitable safety mitigation measures.

### R&D Progress for HCCB TBB

CN HCCB TBM for ITER and CFETR HCCB TBB shall comply with different regulation, French regulation and Chinese regulation, respectively. But from the pressure equipment point view, both regulations and codes have similar requirements. Considering the similarity between CN HCCB TBM for ITER and CFETR HCCB TBB except some features, such as FW armor, coolant pressure, design scheme and size, the R&D results of CN HCCB TBM can be partly used for CFETR HCCB TBB.

### Material Development

CLF-1 steel, tritium breeder and neutron multiplier have been developed based on the requirement of ITER TBM and their fabrication procedures have been preliminarily finalized. The next step is to enlarge production capacity considering the demand of CFETR TBB, which will depend on the time scale of CFETR construction after the decision by the government.

Beyond the ITER, considering the high operation temperature and high energy neutron of fusion reactor and its irradiation damage, the reduced activation ferritic-martensitic (RAFM) steel is not applicable, and then both the TMT (thermomechanical treatments) RAFM and ODS (oxide dispersion strengthened) RAFM steel are promising option for the TBB. Several types of strengthening dispersion CLF-1 steels and CLF-1 steel with Ce rare earth element addition have been investigated [32]. The possible implementation process for ODS CLF-1 steel such as mechanical alloying (MA) followed by hot isostatic pressing (HIP) and selective laser melting (SLM) followed by heat treatment (HT) have been studied [33]. And also, some research about another carbon dispersion strengthen (CDS) such as  $\text{Al}_4\text{C}_3$ ,  $\text{Ti}_3\text{SiC}_2$  and  $\text{Cr}_2\text{AlC}$  has been researched [34]. Figure 31 gives the mechanical properties of these strengthened CLF-1 steel. Based on these researches, the CLF-1 with Ce addition is great way to increase



the strength with no elongation reduction while more research about the high temperature properties shall be evaluated. And for the ODS steel, the strength is not increased obviously, while the creep properties are improved [33].

### Fabrication Processes

Due to the main differences between CN HCCB TBM and CFETR TBB, the size of the components and tungsten armor on the first wall, the developed fabrication processes for TBM cannot be directly used for some larger components of CFETR TBB and additional investigations are needed. These aspects have been covered by the current ongoing R&D activities at SWIP.

The different potential methods for W/CLF-1 steel connection have been investigated, including hot isostatic pressing (HIP), vacuum brazing, laser cladding, physical vapor deposition, vacuum plasma spray and so on. According to the investigation and sample study by inspection and high heat flux test, the HIP and vacuum brazing are selected as the candidate method for W/CLF-1 steel connection due to their good connection quality. Based on this, one small mockup (106 mm × 256 mm) of W/CLF-1 steel connection with the cooling channel has been fabricated by HIP process, which has 10 W tiles (50 mm × 50 mm). After the inspection by UT (ultrasonic testing) and 1000 cycles 1 MW/m<sup>2</sup> high heat flux test by 400 kW HHTF facility, there is not unacceptable defect and damage for W tiles, which preliminarily verifies the feasibility of the HIP process for W/CLF-1 steel connection (Fig. 32). Based on this result, the middle size mockup (220 mm × 940 mm) of W/CLF-1 steel connection is under planned.

Considering the large size of components for CFETR TBB, especially for the FW and cooling plate, several fabrication methods are under investigation. Currently two methods, deep hole drilling + bending and hole drilling + welding, are considered as the most promising procedures for the FW and the process study has been started (Fig. 33). After the fabrication process investigation, one mockup of CFETR HCCB TBB module will be

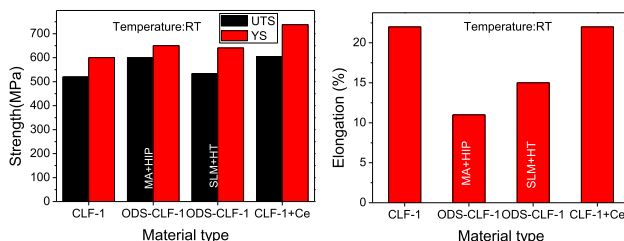


Fig. 31 Mechanical properties of strengthened CLF-1 steel

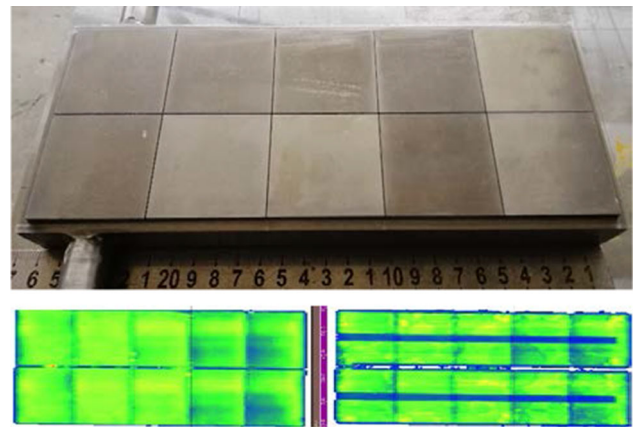


Fig. 32 W/CLF-1 steel connection mockup and its UT result



Fig. 33 Deep hole drilling for Ø6 mm holes in 2 m long plate and its destructive inspection

fabrication to verify the feasibility of whole fabrication procedure.

At the same time, under support of the domestic project for CFETR R&D, the helium cooling hydraulic testing platform (2.5 kg/s, 12 MPa, 500 °C) is under design and will be constructed in the following 2 years, which will be used for the hydraulic testing and safety study of CFETR HCCB TBB mockup.

SWIP is also studying the complex tritium behaviors and interactions in various materials, mainly by simulative experiments with hydrogen and deuterium. A multi-function gas-driven permeation/desorption device is extensively used in SWIP. This device can achieve 1E−7 Pa high vacuum and heat disk-shaped samples to 800 °C. Hydrogen/deuterium permeation and thermal desorption tests can be performed. Another facility under construction is plasma driven permeation facility, which will be installed in the material test window in the recently constructed large size linear plasma device LEAD in SWIP. Plasma driven permeation through samples under hydrogen/deuterium plasma condition will be tested. Ion guns and

nuclear reaction analysis equipment are also planned to be installed in the same plasma device. Ion-irradiation of the sample and deuterium depth profile measurement are expected in future experiments.

## Summary

The development of blanket technology is one of the most important parts of fusion research at SWIP, which focuses on the key technologies for the design, materials, fabrication, inspection and test of blanket for ITER and CFETR.

The ITER EHF FW technologies as regarding to its heat removal capability and thermal fatigue tolerability have been fully demonstrated. The design is updated recently to improve its assembly flexibility and manufacture reliability, and is steadily progressing in verification by R&Ds. The performance and manufacturability of the ITER shielding blocks is verified in the full-scale prototype qualification program, and the series production is in good progress with the solution of hot helium leak test technology at operational temperature and pressure.

The design and R&D of CN HCCB TBS is being implemented based on the ITER schedule. In order to support the design validation, the related R&D activities have been implemented, such as CLF-1 steel and functional materials development, fabrication of semi-prototype TBM module, construction of testing facilities and so on. It will provide the indispensable experience for the design of CFETR TBB [35].

The development of CFETR HCCB TBB is one of the most important activities of CFETR, which is learning from the CN HCCB TBS and ITER. Its preliminary design has been started based on the latest CFETR design. Meanwhile, the pre-R&D for the key technologies, such as W/CLF-1 connection, fabrication processes and testing platforms, are under implementation.

With the constantly advancing of these projects, SWIP is contributing more to overcome these technical challenges faced by blanket in fusion reactor.

**Acknowledgements** This work was supported by the National Key Research and Development Program of China with Grant Numbers 2017YFE0300603, 2017YFE0300601 and 2017YFE0300503.

## Declarations

**Conflict of interest** The views and opinions expressed herein do not necessarily reflect those of the ITER Organization.

## References

1. X.R. Duan et al., Progress in fusion technology at SWIP. *Fusion Eng. Des.* **109–111**, 1022–1027 (2016)
2. L.M. Giancarli et al., ITER TBM program and associated system engineering. *Fusion Eng. Des.* **136**, 815–821 (2018)
3. Y.X. Wan et al., Overview of the present progress and activities on the CFETR. *Nucl. Fusion* **57**, 102009 (2017)
4. G. Zhuang et al., Progress of the CFETR design. *Nucl. Fusion* **59**, 112010 (2019)
5. X.Y. Wang et al., Current design and R&D progress of the Chinese helium cooled ceramic breeder test blanket system. *Nucl. Fusion* **59**, 076019 (2019)
6. X.Y. Wang et al., Preliminary Design and Tritium Assessment of CFETR HCCB TBB, *Paper No. OIB.5, Presented at 12th International Conference on Tritium Science & Technology, Busan, Korea* (2019)
7. H.B. Liao et al., Recent progress of R&D activities on reduced activation ferritic/martensitic steel (CLF-1). *Fusion Eng. Des.* **147**, 111235 (2019)
8. Y.J. Feng, K.M. Feng, Q.X. Cao et al., Current status of the fabrication of Li<sub>4</sub>SiO<sub>4</sub> and beryllium pebbles for CN HCCB TBM in SWIP. *Plasma Sci. Technol* **15**(3), 291–294 (2013)
9. A.R. Raffray, B. Calcagno, P. Chappuis et al., The ITER blanket system design challenge. *Nucl. Fusion* **54**, 033004 (2014)
10. R. Mitteau, B. Calcagno, P. Chappuis et al., The design of the ITER first wal panels. *Fusion Eng. Des.* **88**, 568–570 (2013)
11. K. Ioki, F. Elio, V. Barabashi et al., Six-party qualification program of FW fabrication methods for ITER blanket module procurement. *Fusion Eng. Des.* **82**, 1774–1780 (2007)
12. J.M. Chen, X. Liu, P.H. Wang et al., Progress in developing ITER and DEMO first wall technologies at SWIP. *Nucl. Fusion* **60**, 016005 (2020)
13. K. Wang, J. Chen, P. Wang et al., China's technical achievements on ITER enhanced heat flux first wall in the pre-qualification. *Fusion Eng. Des.* **146**, 2045–2048 (2019)
14. L.M. Giancarli et al., *Overview of Recent ITER TBM Program Activities, Paper No. PL-3, to be Presented at ISFNT-14, Budapest, Hungary* (2019)
15. X.H. Wu et al., Design optimization and analysis of CN HCCB TBM-set. *Fusion Eng. Des.* **136**, 839–846 (2018)
16. L.M. Giancarli et al., Progress and challenges of the ITER TBM Program from the IO perspective. *Fusion Eng. Des.* **109–111**, 1491–1497 (2016)
17. X.H. Wu et al., Preliminary design and structural analysis for HCSB TBM shield module. *Nucl. Fusion Plasma Phys.* **36**(2), 143–147 (2016)
18. Q.X. Cao et al., Neutronic calculation analysis for CN HCCB TBM-Set. *Plasma Sci. Technol.* **17**(7), 607–611 (2015)
19. X.Y. WANG et al., Thermal-hydraulic analysis of HCCB test blanket system. *Fusion Eng. Des.* **138**, 352–357 (2019)
20. D.L. Luo et al., Recent progress of China HCCB TBM tritium system. *Fusion Eng. Des.* **109–111**, 416–421 (2016)
21. B. Zhou et al., Hydraulic analysis for TBM first wall based on CFD method. *Nucl. Fusion Plasma Phys.* **36**(3), 219–223 (2016)
22. X.Y. Wang et al., Study on normal operation and failure of pressure control for CN HCCB TBS primary coolant system. *Fusion Eng. Des.* **144**, 154–159 (2019)
23. Y.L. Wang et al., Preliminary LOFA and in-vessel LOCA analysis for CN HCCB TBS. *Nucl. Fusion Plasma Phys.* **36**(3), 213–218 (2016)
24. Y.L. Wang et al., Preliminary accident analysis for CN HCCB TBS heat exchanger tube rupture. *Nucl. Fusion Plasma Phys.* **36**(4), 328–333 (2016)

25. Y.L. WANG et al., Preliminary accident analyses of in-vessel LOCA and in-box LOCA for China helium-cooled ceramic breeder test blanket system. *Fusion Eng. Des.* **112**, 548–556 (2016)
26. Y.J. Feng, K.M. Feng, J.L. Zhang, Study on REP method for fabrication neutron multiplier beryllium pebbles, *Progress Report on China Nuclear Science & Technology*, vol. 2, pp. 82–87
27. Y.J. Feng et al., Fabrication and characterization of Li<sub>4</sub>SiO<sub>4</sub> pebbles by melt spraying method. *Fusion Eng. Des.* **87**, 753–756 (2012)
28. S.K. Wu et al., Investigation on microstructure and properties of narrow-gap laser welding on reduced activation ferritic/martensitic steel CLF-1 with a thickness of 35 mm. *J. Nucl. Mater.* **503**, 66–74 (2018)
29. C. Wang et al., Microstructure and properties of electron beam welding of low activation ferrite/martensitic steel thick plate. *Mech. Manuf. Abstr. Spec. Res. Weld. Fascicles* **3**, 9–15 (2018)
30. X.F. Ye et al., Design and construction of a small helium loop. *Nucl. Fusion Plasma Phys.* **37**(4), 465–468 (2017)
31. X.H. Wu et al., Optimized design and engineering analyses for HCCB Blanket of CFETR, in *Presented at 27th International Conference of Nuclear Engineering, Tsukuba, Japan* (2019)
32. J. Gong, H.B. Liao, K. Zhang, X.Y. Wang, Heat treatment optimization of China low-activation ferritic/martensitic steel with cerium addition. *Fusion Eng. Des.* **158**, 111696 (2020)
33. S. Yang, J.M. Chen, H.Y. Fu, Mechanical properties and microstructure of 9Cr-ODS-CLF-1 steel. *Fusion Eng. Des.* **151**, 111406 (2020)
34. S. Yang, P.F. Zheng, P.H. Wang, Mechanical properties and thermal stability of carbide dispersion strengthened CLF-1 steel. *Fusion Eng. Des.* **136**, 442–446 (2018)
35. X.Y. Wang et al., Development status of helium cooled ceramic breeder tritium breeding blanket in China, invited oral presentations O1-1.2, in *Presented at 14th International Symposium on Fusion Nuclear Technology, Budapest, Hungary* (2019)

**Publisher's note** Springer Nature remains neutral with regard to jurisdictional claims in published maps and institutional affiliations.